Journal of Materials Chemistry A

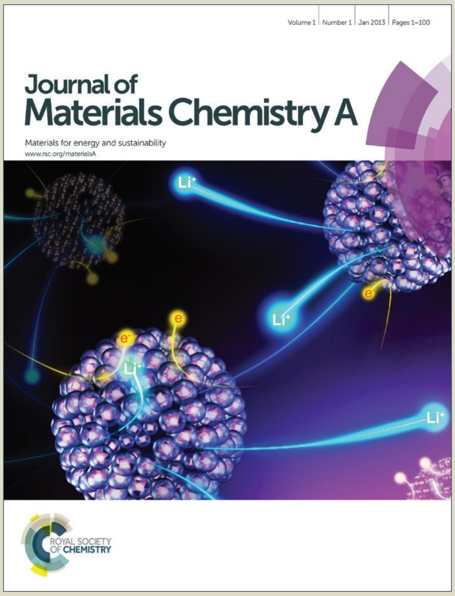

ROYAL SOCIETY OF CHEMISTRY

www.rsc.org/materialsA

Journal Name

COMMUNICATION

Efficient Charge Separation between Bi_2MoO_6 Nanosheets and ZnO Nanowires for Enhanced Photoelectrochemical Properties

Received 00th January 20xx,
Accepted 00th January 20xx

DOI: 10.1039/x0xx00000xwww.rsc.org/

Bingjun Jin,[a,b] Zhengbo Jiao,[a] Yingpu Bi*,[a]

We demonstrate a facile and effective strategy for in-situ growth of Bi_2MoO_6 thin-nanosheets on the well-aligned ZnO nanowires to construct novel hierarchical hetero-arrays, which exhibit excellent visible-light driven photoelectrochemical performances attributed to the highly efficient charge separation between Bi_2MoO_6 nanosheets and ZnO nanowires.

Photoelectrochemical water splitting into hydrogen and oxygen is a promising strategy for renewable energy supply and environmental conservation.[1-4] However, the design and construction of highly efficient semiconductor photoanodes is crucial for its future applications.[5-7] Generally, metal oxides could serve as the promising photoanode materials due to their low-cost synthetic routes and higher stability than other semiconductors such as pure elements and sulfide.[8,9] Among various metal oxides, zinc oxide (ZnO) has attracted extensive attention owing to its low onset potential and high electron mobility.[10-13] Especially, vertically oriented one dimensional (1D) ZnO nanowire arrays have become one of the most intensively studied nanostructures,[14,15] which can offer not only a large surface area but also a short diffusion length to conductive substrate for charge transfer.[16,17] However, limited by the large band gap (3.37 eV) and high recombination ratios, ZnO nanowire arrays generally exhibit low conversion efficiency for the utilization of solar energy, which greatly limited their practical applications.[18-22] To resolve these issues, much effort has been focused on coupling ZnO nanowire arrays with other semiconductors, such as $BiVO_4$, CdS, and CdSe owning their excellent visible-light absorption and suitable energy levels, for facilitating the charge separation and enhancing their visible-light photoelectrochemical (PEC) performances.[23-27] However, note that traditional particles of these semiconductors were usually decorated on ZnO nanowires, which greatly restricts their visible-light absorption efficiency due to the relatively low surface areas. Compared with 0D nanoparticles, the rational design and construction of 2D semiconductor thin-nanosheets on ZnO nanowires to form hierarchical hetero-arrays may be more feasible for capturing light and improving the charge separation, and will exhibit the enhanced photoelectrochemical efficiency.

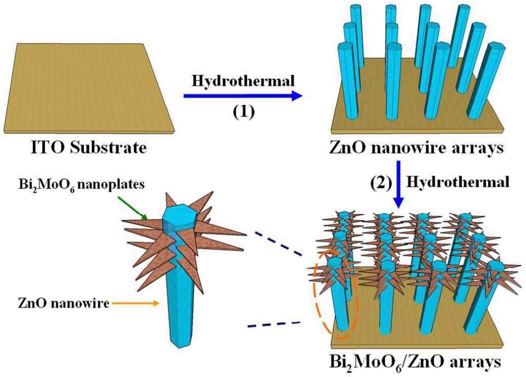

Scheme 1 Schematic illustration of the synthesis approach of frame structure Bi_2MoO_6/ZnO hierarchical hetero-structure based on ZnO nanowire arrays.

Herein, we have demonstrated a simple hydrothermal process for the rational construction of 2D Bi_2MoO_6 thin-nanosheets on the well-aligned ZnO nanowire arrays to construct hierarchical hetero-nanoarrays. Benefiting from unique hierarchical structures, the as-prepared Bi_2MoO_6 nanosheets modified ZnO nanowire arrays could achieve a high photocurrent density of 110 $\mu A \cdot cm^{-2}$ at 0.2V vs. SCE under visible-light illumination, nearly two orders of magnitude larger than that of both Bi_2MoO_6 and ZnO. Furthermore, visualized evidence for efficient charge separation and electron transfer from Bi_2MoO_6 nanosheets to ZnO nanowires has been achieved by using a powerful in-situ XPS technique. More importantly, these demonstrations provide further insight for improving the efficiency of semiconductors by using a suitable electron transfer channels, which may be promising for rational construction of solar conversion and storage devices.

---

[a] *State Key Laboratory for Oxo Synthesis & Selective Oxidation, and National Engineering Research Center for Fine Petrochemical Intermediates, Lanzhou Institute of Chemical Physics, CAS, Lanzhou 730000, China. E-mail: yingpubi@licp.cas.cn.*
[b] *Lanzhou University of technology, Lanzhou 730050, China.*

† Electronic Supplementary Information (ESI) available: Experimental procedure, and additional Figures. See DOI: 10.1039/x0xx00000x

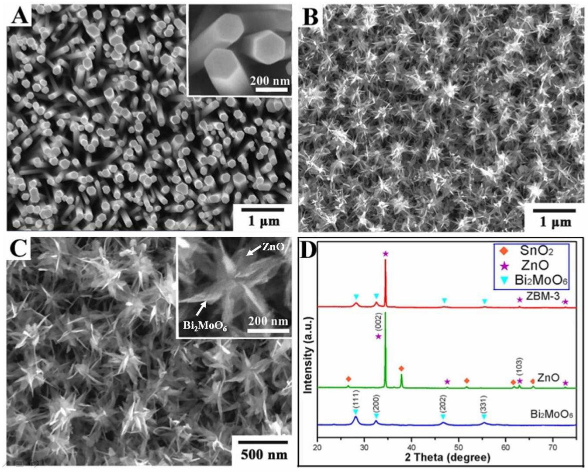

Fig. 1 (A) Top-view SEM images of ZnO nanowire arrays, (B and C) Top-view SEM images of the Bi_2MoO_6/ZnO hetero-structure (with 0.003M Bi_2MoO_6 which noted as ZBM-3), (D) XRD patterns of ZnO nanowire arrays, pure Bi_2MoO_6 and ZBM-3.

Controllable construction of Bi_2MoO_6 nanosheets on the ZnO nanowires arrays was achieved through a two-step hydrothermal method, and a schematic illustration on the synthetic procedure was shown in Scheme 1. Fig. 1A shows the typical scanning electron microscope (SEM) images of as-prepared ZnO nanowire arrays by the first-step hydrothermal method. It is obviously revealed that the obtained ZnO nanowire arrays are well aligned and have a hexagon cross-section with an average width of about 200 nm. When the product was used as the growth template for the further hydrothermal reaction, interestingly, numerous thin Bi_2MoO_6 nanoplates grown on the top regions of ZnO nanowires to formed a novel windmill-like hetero-structure (Fig. 1B). More specifically, the enlarged SEM image (Fig. 1C) clearly reveals that this windmill-like structure is constructed by inter-crossed nanosheets with the main diameters of 200-300 nm (inset of Fig. 1C). Furthermore, their crystalline structure as well as compositions has been determined by the X-ray diffraction (XRD). For comparison, both pure ZnO anowire arrays and Bi_2MoO_6 nanoplates have also been tested and shown in Fig. 1D. It can be seen that the main diffraction peaks at 34.4°, 62.9° and 72.6° could be indexed to the (002), (103) and (004) crystal faces of hexagonal ZnO (JCPDS 05-0664), respectively. Besides, four distinctive peaks with 2θ values of 28.2°, 32.4°, 46.7° and 55.3° were observed in Bi_2MoO_6/ZnO hetero-structure (ZBM-3), matched well with (111), (200), (202) and (331) crystal planes of koechlinite Bi_2MoO_6 (JCPDS 21-0102). The above XRD results illustrate that the hetero-structure is composed of ZnO and Bi_2MoO_6, which is in good agreement with the SEM results. The chemical state of elements and bonding environment of the Bi_2MoO_6/ZnO hetero-structure were further performed by X-ray photoelectron spectroscopy (XPS). The fully scanned spectra (Fig. S3A) clearly demonstrates the presence of Zn, O, Mo and Bi elements in the obtained hetero-structure. The wide and asymmetric peak of the high-resolution O 1s spectrum (Fig. S3B) could be fitted with four peaks. More specifically, the peak at 532.0 eV is attributed to the O-H bond due to absorbed H_2O molecules, and the other three peaks at 530.9, 530.1 and 529.7 eV were indexed to Mo-O, Zn-O and Bi-O bonds, respectively.[28,29] Fig.S3C, S3D and S3E present the high-resolution spectra of Zn 2p, Mo 3d and Bi 4f in the Bi_2MoO_6/ZnO heterostructure (ZBM-3), and Zn^{2+}, Mo^{6+} and Bi^{3+} species were confirmed in the as-prepared samples according to the peak positions. On the basis of above results, it can be concluded that the Bi_2MoO_6 have been successfully constructed on the ZnO nanowire arrays.

Furthermore, morphologies and compositions of the Bi_2MoO_6/ZnO hetero-structures could be rationally tailored by simply adjusting the concentrations of both $Bi(NO_3)_3{\cdot}5H_2O$ to $Na_2MoO_4{\cdot}2H_2O$, and the corresponding SEM images and XRD patterns were showed in Fig. S1 and Fig. S2, respectively. It can be clearly seen that, reducing their concentration, only Bi_2MoO_6 nanoparticles were formed on the ZnO nanowire arrays, and the diameter of ZnO nanowire had been gradually decreased (Fig. S1B and S1C). In contrast, the amounts of Bi_2MoO_6 nanosheets in the obtained hetero-structures greatly increased (Fig. S4D). Further increasing their concentrations, all the ZnO nanowires have been completely covered by Bi_2MoO_6 nanosheets. Moreover, the corresponding XRD patterns shown in Fig. S2 clearly reveal that the compositions of all as-prepared samples are exactly consistent. In other words, adjusting of the precursor concentration does not influence the crystal structure of Bi_2MoO_6/ZnO hetero-structure. Therefore, it can be concluded that in the present fabrication system, the precursor amounts play a decisive role for adjusting the morphologies as well as combination modes of Bi_2MoO_6/ZnO hetero-structures.

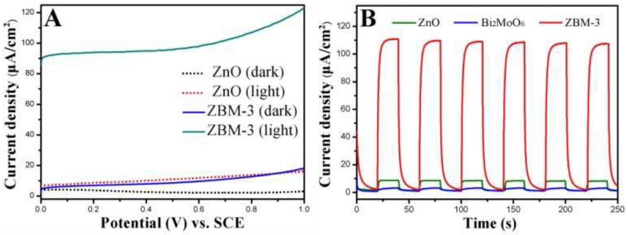

Fig. 2 (A) Linear sweep voltammograms of ZnO nanowire arrays and Bi_2MoO_6/ZnO hetero-structure (ZBM-3) in the dark and under visible light illumination, respectively; (B) Amperometric I–t curves of ZnO nanowire arrays, pure Bi_2MoO_6 and ZBM-3 at an applied voltage of +0.2 V with 20 s light on/off cycles.

To further evaluate the PEC properties of the as-prepared Bi_2MoO_6/ZnO heterostructures, systematic PEC measurements were carried out under visible-light irradiation (λ > 420 nm). For comparison, PEC properties of pure ZnO nanowire arrays and Bi_2MoO_6 have also been investigated. As shown in Fig. 2A, a set of linear sweep voltammetry (LSV) in the dark and visible light irradiation has been studied. Comparing with the pure ZnO and Bi_2MoO_6, the photocurrent of Bi_2MoO_6/ZnO hetero-structures increased significantly. In addition, we performed amperometric I-t curves under transient illumination at applied voltage of +0.2V to examine the photo-response vs time. As shown in Fig. 2B, the photocurrent value of the Bi_2MoO_6/ZnO hetero-structure can reach up to 110 μA·cm^{-2}, which is much higher than that of the ZnO nanowire arrays (9 μA·cm^{-2}) and pure Bi_2MoO_6 (4 μA·cm^{-2}). Because the magnitude of the photocurrent can represent the charge collection efficiency of the electrode surface, the high value indicates that the novel Bi_2MoO_6/ZnO hierarchical hetero-structure can greatly enhance the PEC properties (see Scheme 2). The electrochemical impedance spectra (EIS) Nyquist plots (Fig. S6) clearly reveal that Bi_2MoO_6/ZnO hetero-structure shows smaller semicircle at high frequencies as compared with ZnO nanowire arrays and pure Bi_2MoO_6 nanosheets, suggesting that the hetero-structures possess faster transport rate of charge carriers. At the same time, the stability test (Fig. S8) had been performed and clearly shows that the photocurrent density of the as-prepared Bi_2MoO_6/ZnO hetero-structure kept relatively constant under continuous visible light illumination, demonstrating the excellent photoelectric durability. Moreover, photocurrent responses under a certain monochromatic light irradiation have also been tested (Fig. S9). Compared with both pure ZnO and Bi_2MoO_6, the photocurrent density of Bi_2MoO_6/ZnO hetero-structure was largely enhanced after 400 nm, which shows that this hetero-structure has more excellent photoelectric properties in the visible light range.

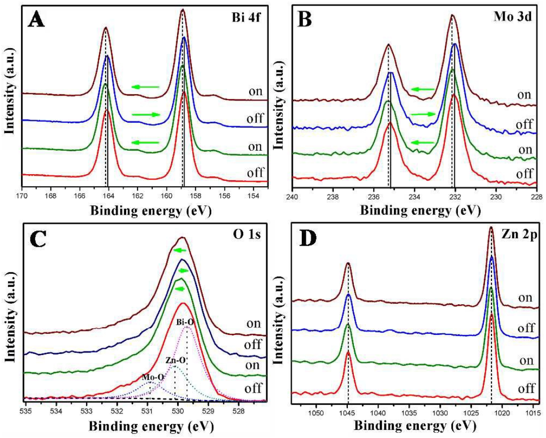

Fig. 3 (A) In situ Zn 2p XPS spectra (B) In situ Mo 3d XPS spectra, (C) In situ Bi 4f XPS spectra (D) In situ O 1s XPS spectra of Bi_2MoO_6/ZnO hetero-structure (ZBM-3) under visible light with on/off cycles.

In order to reveal the charge separation and electron transfer between the ZnO nanowire arrays and Bi_2MoO_6 nanosheets, a novel in-situ XPS technique was firstly performed to follow the evolution of binding energies under transient visible light illumination. As can be seen in Fig. 3A, before the irradiation, two strong peaks at 164.28 eV and 158.9 eV which are indexed to Bi $4f_{5/2}$ and Bi $4f_{7/2}$, which demonstrates that bismuth species in the hetero-structure is Bi^{3+}. Amazingly, the peak emerged a remarkable shift to right (BE become larger) when the sample was irradiated by visible-light, but returning to the original position when light off. Moreover, similar phenomena of the photoinduced shift of Mo 3d could be also observable (Fig. 3B). As for the O 1s, three lattice Bi-O bonds at 529.7 eV and Mo-O bonds at 530.9 eV, in agree the same change with Fig. 3A and Fig. 3B, while Zn-O bond keep a fixed position without any change (Fig. 3D). On the basis of above results, it can be concluded that under visible light irradiation, the photoexcited electrons over Bi_2MoO_6 were rapidly transferred to the ITO substrate through the aligned ZnO nanowire arrays, and abundant holes left behind in Bi_2MoO_6 nanosheets, which make the binding energies of Bi, Mo and O elements increase and shift to the same direction under in-situ XPS measurements.

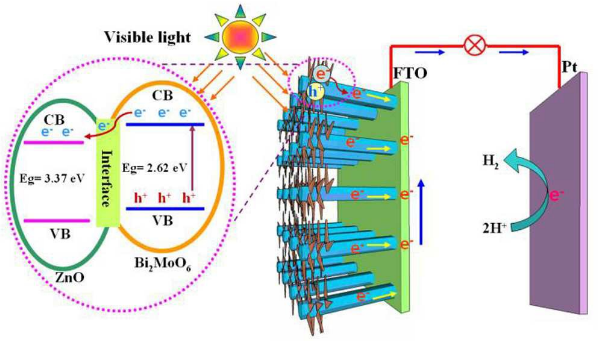

Scheme 2 Schematic illustration for the charge separation and transport of the Bi_2MoO_6/ZnO hetero-structure.

According to the results discussed above, we propose a possible mechanism for the improved charge separation of Bi_2MoO_6/ZnO hetero-structure nanowire arrays under visible light irradiation. As shown in Scheme 2, under visible light illumination (λ>420 nm, energy less than 2.95 eV), Bi_2MoO_6 with narrow band gap energy (2.62 eV) could be easily excited and induce the generation of photoelectrons and holes, while ZnO could not be excited due to its wide energy gap of about 3.2 eV.[30] Electrons of Bi_2MoO_6 are photoexcited from the valence band to the conduction band and then transferred to the conduction band of ZnO because the conduction band of Bi_2MoO_6 is more negative than that of ZnO.[31] At the same time, the aligned ZnO nanowire arrays provide a conduction path for electron transfer to conductive substrate. So the electrons come from Bi_2MoO_6 will be rapidly transferred to the ITO along the vertically oriented ZnO nanowires. Moreover, the formed junction between ZnO and Bi_2MoO_6 in the hetero-structure could further prevent the recombination of photoelectrons and holes. In such a way, photoinduced electron–hole pairs could be effectively separated and thus enhance the photoconversion efficiency.

In summary, we demonstrated a facile hydrothermal process for fabricating the Bi_2MoO_6 nanosheets/ZnO nanowire hierarchical hetero-arrays for the first time. Moreover, the relative performance tests indicated that the visible-light driven PEC properties of Bi_2MoO_6/ZnO hetero-arrays have been greatly improved nearly two orders of magnitude compared with pure Bi_2MoO_6 nanosheets and ZnO nanowire arrays. Furthermore, direct observation of rapid charge separation and transfer between Bi_2MoO_6 nanosheets and ZnO nanowires has been achieved by a powerful in-situ XPS technique. We believe that this strategy may be applied in constructing other ZnO nanowire based hierarchical architecture as well as nano-devices for solar photoelectric conversion.

Acknowledgements

This work was supported by the "Hundred Talents Program" of the Chinese Academy of Science and National Natural Science Foundation of China (21273255, 21303232, 21573264).

Notes and references

1 Z. G. Zou, J. H. Ye, K. Sayama and H. Arakawa, *Nature*, 2001, **414**, 625-627.
2 O. Khaselev and J. A. Turner, *Science*, 1998, **280**, 425-427.
3 M. R. Hoffmann, S. T. Martin, W. Choi and D. W. Bahnemannt, *Chem. Rev.*, 1995, **95**, 69-96.
4 X. Chen, S. Shen, L. Guo and S. Mao, *Chem. Rev.*, 2010, **110**, 6503–6570.
5 P. K. Santra and P. V. Kamat, *J. Am. Chem. Soc.*, 2012, **134**, 2508–2511.
6 B. D. Alexander, P. J. Kulesza, I. Rutkowska, R. Solarska and J. Augustynski, *J. Mater. Chem.*, 2008, **18**, 2298-2303.
7 N. S. Lewis, *Science*, 2007, **315**, 798-801.
8 N. Pinna, G. Neri, M. Antonietti and M. Niederberger, *Angew. Chem. Int. Ed.*, 2004, **43**, 4345–4349.
9 G. K. Mor, K. Shankar, M. Paulose, O. K. Varghese, C. A. Grimes, *Nano Lett.*, 2006, **6**, 215-218.
10 Z. Wang, J. Song, *Science*, 2006, **312**, 242-246.
11 F. Xu, Y. Lu, L. Sun, L. Zhi, *Chem. Commun.*, 2010, **46**, 3191-3193.
12 H. Wang, X. Zhang, X. Fan, C. Lee and S. Lee, *Chem. Commun.*, 2009, **39**, 5916-5918.
13 J. Ryu, S. H. Lee, D. H. Nam and C. B. Park, *Adv. Mater.*, 2011, **23**, 1883-1888.
14 S. Xu and Z. L. Wang, *Nano Res.*, 2011, **4**, 1013–1098.
15 Q. Wan, Q. Li, Y. Chen, T. Wang, X. He, J. Li and C. Lin, *Appl. Phys. Lett.,* 2004, **84**, 3654-3656.
16 Z. Yin, Z. Wang, Y. Du, X. Qi, Y. Huang, C. Xue and H. Zhang, *Adv. Mater.*, 2012, **24**, 5374.
17 T. Zhang, W. Dong, M. Keeter-Brewer, S. Konar, R. N. Njabon and Z. R. Tian, *J. Am. Chem. Soc.*, 2006, **128**, 10960.
18 A. Dr. and Y. H. Leung, *Small*, 2006, **2**, 944-961.
19 A. Mclaren, T. Valdes-Solis, G. Li, S. C. Tsang, *J. Am. Chem. Soc.,* 2009, **131**, 12540-12541.
20 S. Cho, J.-W. Jang, J. Kim, J. S. Lee, W. Choi, K.-H. Lee, *Langmuir*, 2011, **27**, 10243-10250.
21 T. Wang, R. Lv, P. Zhang, C. Li and J. Gong, *Nanoscale*, 2015, **7**, 77-81.
22 N. Wang, C. Sun, Y. Zhao, S. Zhou, P. Chen and L. Jiang, *J. Mater. Chem.,* 2008, **18**, 3909-3911.
23 D. R. Baker, P. V. Kamat, *Adv. Funct. Mater.*, 2009, **19**, 805-811.
24 A. Kongkanand, K. Tvrdy, K. Takechi, M. Kuno and P. V. Kamat, *J. Am. Chem. Soc.,* 2008, **130**, 4007-4015.
25 S. J. A. Moniz, J. Zhu and J.W. Tang, *Adv. Energy Mater.*, 2014, **4**, 1301590.
26 S. J. A. Moniz, J. Zhu and J.W. Tang, *Adv. Energy Mater.*, 2014, **4**, 1301590.
27 M. Seol , H. Kim , Y. Tak and K. Yong, *Chem. Commun.*, 2010, **46**, 5521-5523.
28 M. Futsuhara, K. Yoshioka and O. Takai, *Thin Solid Films*, 1998, **322**, 274-281.
29 M. Futsuhara, K. Yoshioka and O. Takai, *Thin Solid Films*, 1998, **322**, 274-281.
30 Z. Zheng, W. Xie, Z. S. Lim, L. You and J. Wang, *Scientific reports*, 2014, **4**. DOI: 10.1038/srep05721.
31 M. Long, W. Cai and H. Kisch, *Chemical Physics Letters*, 2008, **461**, 102-105.

Efficient Charge Separation between Bi_2MoO_6 Nanosheets and ZnO Nanowires for Enhanced Photoelectrochemical Properties

Bingjun Jin, Zhengbo Jiao, Yingpu Bi*

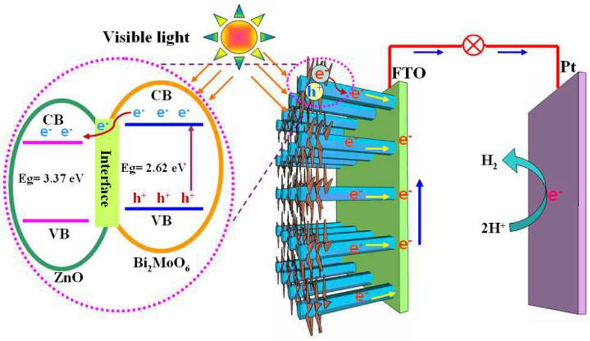

We demonstrate a facile and effective strategy for in-situ growth of Bi_2MoO_6 thin-nanosheets on the well-aligned ZnO nanowires to construct novel hierarchical hetero-arrays, which exhibit excellent visible-light driven photoelectrochemical performances attributed to the highly efficient charge separation between Bi_2MoO_6 nanosheets and ZnO nanowires.